The American Journal of Pathology, Vol. 180, No. 2, February 2012

DOI: 10.1016/j.ajpath.2011.10.035

Matrix Pathobiology

Chop (Ddit3) Is Essential for D469del-COMP Retention and Cell Death in Chondrocytes in an Inducible Transgenic Mouse Model of Pseudoachondroplasia

Karen L. Posey,* Francoise Coustry,*
Alka C. Veerisetty,* Peiman Liu,*
Joseph L. Alcorn,* and Jacqueline T. Hecht*†

From the Department of Pediatrics, University of Texas Medical School at Houston, Houston; and the Shriners Hospital for Children,† Houston, Texas*

Cartilage oligomeric matrix protein (COMP), a secreted glycoprotein synthesized by chondrocytes, regulates proliferation and type II collagen assembly. Mutations in the COMP gene cause pseudoachondroplasia and multiple epiphyseal dysplasia. Previously, we have shown that expression of D469del-COMP in transgenic mice causes intracellular retention of D469del-COMP, thereby recapitulating pseudoachondroplasia chondrocyte pathology. This inducible transgenic D469del-COMP mouse is the only *in vivo* model to replicate the critical cellular and clinical features of pseudoachondroplasia. Here, we report developmental studies of D469del-COMP-induced chondrocyte pathology from the prenatal period to adolescence. D469del-COMP retention was limited prenatally and did not negatively affect the growth plate until 3 weeks after birth. Results of immunostaining, transcriptome analysis, and qRT-PCR suggest a molecular model in which D469del-COMP triggers apoptosis during the first postnatal week. By 3 weeks (when most chondrocytes are retaining D469del-COMP), inflammation, oxidative stress, and DNA damage contribute to chondrocyte cell death by necroptosis. Importantly, by crossing the D469del-COMP mouse onto a *Chop* null background (*Ddit3* null), thereby eliminating Chop, the unfolded protein response was disrupted, thus alleviating both D469del-COMP intracellular retention and premature chondrocyte cell death. Chop therefore plays a significant role in processes that mediate D469del-COMP retention. Taken together, these results suggest that there may be an optimal window before the induction of significant D469del-COMP retention during which endoplasmic reticulum stress could be targeted. *(Am J Pathol 2012, 180:727–737; DOI: 10.1016/j.ajpath.2011.10.035)*

Cartilage oligomeric matrix protein (COMP) is an extracellular matrix (ECM) protein found primarily in cartilage and other musculoskeletal tissues.[1–10] The *COMP* gene (previously *PSACH*; also known as *TSP5*) is the fifth member of the thrombospondin family and is a homopentamer.[1–7] It is composed of a N-terminal pentamerization domain, four EGF-like repeats, seven type II calcium-binding repeats, and a C-terminal globular domain.[7] COMP has several potential functions including interacting with other ECM molecules in the matrix, regulating type II collagen fibril assembly, and enhancing chondrocyte attachment and proliferation.[11–17]

Mutations in COMP, which result in protein misfolding and intracellular retention, cause two autosomal dominant skeletal dysplasias: pseudoachondroplasia, a severe dwarfing condition, and multiple epiphyseal dysplasia (MED/EDM1), a milder disorder.[18–23] Children with pseudoachondroplasia have normal birth parameters, but develop a waddling gait and have decelerating linear growth by 2 to 3 years of age.[24,25] Bone abnormalities develop over time and include shortened limbs, brachydactyly, and pectus carinatum.[24,25] Early-onset osteoarthritis, affecting all of the joints, causes chronic pain, often necessitating hip replacement in early adulthood.[25] Although natural history studies have defined the clinical progression of the pseudoachondroplasia phenotype, little is known about the mechanism or mechanisms underlying the chondrocyte cellular phenotype that causes the diminished bone growth. Most information about the *in vivo* state is derived from bone biopsies of the pseudoachondroplasia growth plate or from *in vitro* tissue culture studies, and thus provides little mechanistic information.

Supported by NIH grant 1R01AR057117 (J.T.H. and J.L.A.), a Shriners Hospital for Children grant (J.T.H.), and the Leah Lewis Foundation.

Accepted for publication October 23, 2011.

Address reprint requests to Jacqueline T. Hecht, Ph.D., Department of Pediatrics, University of Texas Medical School, 6431 Fannin St., Houston, TX 77030. E-mail: Jacqueline.T.Hecht@uth.tmc.edu.

Growth-plate chondrocytes from both pseudoachondroplasia and MED/EDM1 patients show giant rough endoplasmic reticulum (rER) cisternae containing COMP and other ECM proteins [collagen types II and IX and matrilin 3 (MATN3)] that form an ordered matrix network.[2,13,19–40] The inability of mutant COMP to fold properly traps the protein in the ER, thereby allowing intracellular matrix assembly.[23,35,36,41] These matrix-filled cisternae occupy most of the chondrocyte cellular volume, ultimately compromising chondrocyte cellular function and causing premature chondrocyte cell death.[13,18,19,27,32,35,36,39,41]

Earlier pseudoachondroplasia mouse models have not faithfully recapitulated the chondrocyte phenotype and thus have not allowed for analysis of growth plate pathology during skeletal development.[42,43] To circumvent this problem, we generated an inducible transgenic D469del-COMP mouse that we have shown reproduces the characteristic pseudoachondroplasia chondrocyte pathology by 1 month of age, including intracellular retention of COMP, types II and IX collagens, and MATN3, as well as premature intracellular ECM assembly, growth plate abnormalities, and increased numbers of apoptotic chondrocytes.[44] Here, we define the mechanism of chondrocyte loss and ontogeny of D469del-COMP retention and cell death during prenatal and postnatal skeletal development. Most importantly, we show that, in the absence of Chop, D469del-COMP is not retained and D469del-COMP-induced cell death is eliminated.

Materials and Methods

Generation of Constructs

Two plasmids, pTRE-COMP and pTET-On-ColII, were generated as described previously[44] and were used to produce bigenic mutant D469del-COMP mice. Briefly, the pTRE-COMP construct contains the coding sequence of the human *COMP* (+FLAG tag) gene driven by the tetracycline responsive element (TRE) promoter. The pTET-On-ColII construct contains the rtTA coding sequence driven by a type II collagen promoter.[45]

Generation of Bigenic Mice

Standard breeding was used to generate bigenic animals. Genotypes of the transgenic offspring were verified using human COMP and rtTA-specific primers. Mice were pre- and postnatally administered doxycycline (500 ng/mL) through drinking water (supplemented with 5% sucrose). All animal studies were approved by the Animal Welfare Committee of the University of Texas Medical School at Houston.

Generation of Chop Null Bigenic Mice

Chop null mice were procured from Jackson Laboratories and mated with D469del-COMP bigenic mice to obtain a strain expressing D469del-COMP in a *Chop* null background.[46] Genotypes of the *Chop* null mice were verified using Chop-specific primers.[46]

Growth Plate Analysis

Upper tibial growth plates were obtained from at least 10 different mice of each strain. Chondrocytes were counted by marking each chondrocyte using Image-Pro software version 4 (Media Cybernetics, Silver Spring, MD) at ×4 magnification to visualize the entire growth plate. Five measurements along the width of the growth plate were obtained from different limbs, and the measurements were then averaged as previously described.[47]

Immunohistochemistry

Hind limbs of D469del-COMP and C57BL/6 control mice were collected and tibial growth plates were analyzed as previously described.[44] Briefly, the limbs were fixed in 95% ethanol for immunostaining for COMP [rabbit polyclonal antibody, 1:200 (Kamiya, Seattle, WA) or ab11056-rat antibody, 1:100 (Abcam Cambridge, MA)], FLAG (Abcam, Cambridge, MA), PCNA [93–1143 (Invitrogen, Carlsbad, CA)], AIF [4642, 1:50 (Cell Signaling Technology, Danvers, MA)], and H2AX [9718, 1:100 (Cell Signaling)] or in 10% formalin for TUNEL staining. The COMP rabbit antibody cross-reacts with both endogenous mouse and transgenic human COMP, whereas the COMP rat antibody is specific for human COMP. FLAG specifies the recombinant human D469del-tagged COMP.

Retention Scoring

A scoring strategy was devised to measure the relative amount of D469del-COMP retention in the growth-plate chondrocytes of transgenic mice. Growth plates were processed as described above and as described previously.[47] Each chondrocyte in the visual field of images at ×400 magnification was scored for retention in 10 separate images. The scorer visually estimated the size of D469del-COMP accumulation area, compared with the area of the nucleus for each chondrocyte. An average score was calculated from these images. Chondrocytes were scored as follows: 1 = no retention, 2 = retention area is less than that of the nucleus, 3 = retention area is the same size as the nucleus, and 4 = retention area is larger than the nucleus in each chondrocyte.

RNA Extraction and Real-Time qRT-PCR

Mice of various ages were collected and soft tissue was removed from the skeleton at age embryonic day 15.5 (E15.5), or knee and elbow joints at postnatal day 1 (P1), or knee joint at all other ages. Tissue was immediately homogenized in TRIzol reagent (Sigma-Aldrich, St. Louis, MO) and RNA was extracted according to the manufacturer's protocol. Quantitative real-time RT-PCR (qRT-PCR) was performed using an ABI 7700 sequence detector (Applied Biosystems, Foster City, CA). DNA was removed using amplification grade DNase (Invitrogen) according to the manufacturer's instructions. Each assay was replicated three times, and each sample was measured in triplicate, including a control without reverse transcriptase. The final data were normalized to Hprt1 ×

100 (percentage of the normalizer transcript). qRT-PCR was performed using standard methods and the following primers: Grp78 5′-CATGGTTCTCACTAAAATGAAGG-3′ and 5′-GTAAGCTGGTACAGTAACAACTG-3′; Xbp-1 5′-GTCTGCTGAGTCCGCAGCAGGT-3′ 5′-CAGACTCAGAATCTGAAGAGGC-3′; Edem1 5′-AGTCAAATGTGGATATGCTACGC-3′ 5′-ACAGATATGATATGGCCCTCAGT-3′; Chop 5′-TGCCTTTCACCTTGGAGAC-3′ and 5′-CGTTTCCTGGGGATGAGATA-3′; Ero1B 5′-CGTCCTTTAAATCCTTTGGCG-3′ and 5′-ACACAAACCTTCTAGCCACG-3′; GADD34 5′-AGAGAAGCCAGAATCACCTTG-3′ and 5′-ACTGTGACTTTCTCAGCGAAG-3′; GADD45A 5′-CCGAAAGGATGGACACGGTG-3′ and 5′-TTATCGGGGTCTACGTTGAGC-3′; and Hprt1 (normalizer) 5′-CCTCATGGACTGATTATGGACAG-3′ and 5′-TCAGCAAAGAACTTATAGCCCC-3′.

Microarray Analysis

Total RNA (300 ng) from both hind-limb knee joints of each sample was purified using TRIzol reagent and RNeasy columns (Qiagen, Valencia, CA). RNA was amplified using a total prep RNA amplification kit (Illumina, San Diego, CA). RNA was assessed by RNA integrity number (RIN number), and type II collagen was assessed to verify that both the C57BL/6 and D469del-COMP RNA preparations were primarily from chondrocytes. For each time point, three control and three D469del-COMP animals were examined, to control for variation in expression. *In vitro* transcription was performed and biotinylated cRNA was synthesized by 14-hour amplification with dNTP mix containing biotin-dUTP and T7 RNA polymerase. Amplified cRNA was subsequently purified and concentration was measured. An aliquot of 1.5 μg of amplified products was loaded onto Illumina Sentrix BeadChip mouse WG-6.v2 arrays, hybridized at 58°C in an Illumina hybridization oven for 17 hours, washed, and incubated with streptavidin-Cy3 to detect biotin-labeled cRNA on the arrays. Arrays were dried and scanned with an Illumina BeadArray reader.

Data were analyzed using Illumina GenomeStudio software. Clustering and pathway analysis were performed with GenomeStudio and Ingenuity Pathway Analysis software (Ingenuity Systems, Redwood City, CA), respectively. A P value of <0.05 was considered significant.

The mRNAs were classified into functional categories.

Limb Length Measurements

Hind limbs were obtained from 12 control and 12 D469del-COMP mice and the soft tissue was removed. The skeleton was stored in 70% ethanol and then subjected to radiographical examination. The limbs were attached to a grid to ensure consistency and accuracy of measurements. Measurements were made from end to end on both long bones in the hind limb, using Image-Pro software, as previously described.[47] A t-test was used to compare tibial measurements from control and D469del-COMP mice limbs.

Skeletal Preparations

Mice were collected and the soft tissue removed and then fixed overnight in 95% ethanol. Skeletons were stained for 48 hours with Alcian Blue (0.015% solution in 20% acetic acid and 80% methanol), then transferred to 95% ethanol for 2 hours, and then to 2% KOH for 3 hours. The mineralized bone was then stained with Alizarin Red (0.005% in 1% KOH) for 3 hours. The skeleton was cleared in 1% KOH in 20% glycerol for 48 hours and then stored in a glycerol ethanol mixture (1:1).

Results

D469del-COMP Growth Plates Become Disorganized and Thinner during Juvenile Development

We first asked whether the presence of D469del-COMP in our transgenic mouse causes growth plate abnormalities over time. The growth plate organization was similar in D469del-COMP and control mice until 2 weeks (P14; Figure 1, A–C and G–I). At 3 weeks (P21; Figure 1, D and J), more acellular gaps were seen and the growth plate was thinner than control (Figure 1, M and N). By 4 weeks, the growth plate continued to be thinner, compared with control, and loss of chondrocytes was evident (Figure 1, E, K, M, and N). At 2 months, when skeletal growth is complete, the D469del-COMP growth plate had very few chondrocytes, unlike the control (Figure 1, F and L). Changes in the D469del-COMP growth plate are attributed to expression of D469del-COMP rather than to doxycycline exposure, because all mice were subjected to the same doxycycline treatment. These results indicate that D469del-COMP expression causes loss of growth-plate chondrocytes, which is evident by 3 weeks of age. There

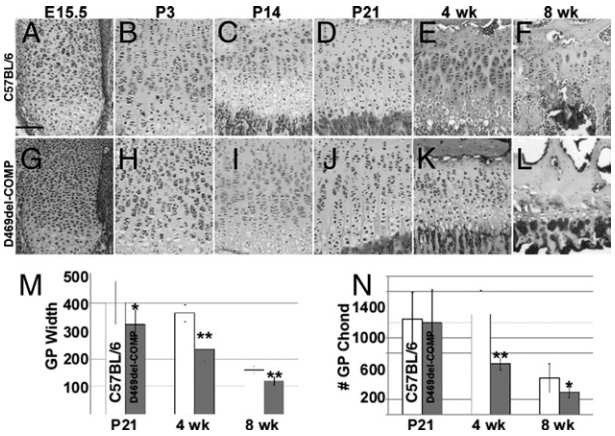

Figure 1. Histomorphometric analysis of D469del-COMP growth plates from E15 to 2 months of age. H&E staining of growth plates at various ages in control C57BL/6 (**A–F**) and D469del-COMP (**G–L**) mice. D469del-COMP and control growth plates are similar until P14 (**D** and **J**), when the growth plates of D469del-COMP mice are more disorganized. Original magnification, ×20 (**A–L**). **M:** Quantification of growth plate width. Growth plates from D469del-COMP mice are narrower than those of controls at P21, 1 month, and 2 months of age. **N:** Quantification of number of chondrocytes. Fewer chondrocytes are present in the D469del-COMP growth plate, compared with controls, at 1 and 2 months of age. $^{*}P \leq 0.05$, $^{**}P \leq 0.01$.

is little change in the number of chondrocytes and growth plate height before this developmental time point.

D469del-COMP Retention Is First Evident in Prenatal Growth-Plate Chondrocytes

We next asked when D469del-COMP becomes retained in the chondrocytes of the developing growth plate. Previously, we showed that D469del-COMP is retained in the rER and forms an ordered intracellular matrix composed of collagens types II and IX and MATN3 in growth plates from 1-month-old mice, identical to what is observed in pseudoachondroplasia patient chondrocytes.[21,44] In these studies, a FLAG antibody recognizes the transgenic D469del-COMP-FLAG protein and a COMP antibody recognizes both the endogenous murine and transgenic human COMP-FLAG. Few chondrocytes showed intracellular retention at E15, compared with control (Figure 2, A and G). Both the D469del-COMP and control chondrocytes show a patchy distribution of COMP (Figure 2, A and G). Intracellular retention was measured using the scoring methodology described under *Materials and Methods* and presented schematically in Figure 2M (an example of D469del-COMP growth-plate chondrocytes with a retention score of 4 is presented in Figure 2N). The intracellular retention increases, with many chondrocytes showing retention by P3; almost all chondrocytes are retaining D469del-COMP by P21 (Figure 2, B–D and O); In comparison, in the nontransgenic controls, all endogenous COMP is extracellular (Figure 2, G–L). This indicates that intracellular retention is a progressive process with the maturing of the growth plate and eventually encompasses all chondrocytes in the growth plate.

To quantitate the progression of D469del-COMP retention, we developed a scoring system based on the area of the COMP-positive intracellular retention relative to the area of the nucleus as defined by DAPI staining (Figure 2B). This system was designed to compare the relative amount of D469del-COMP retained in growth-plate chondrocytes at different developmental ages. There was a significant increase in D469del-COMP retention starting shortly after birth (P3), compared with that seen at E15.5 (Figure 2B). D469del-COMP retention continued to increase significantly up to P14, at which point the levels remained relatively constant, suggesting that a steady state level had been attained.

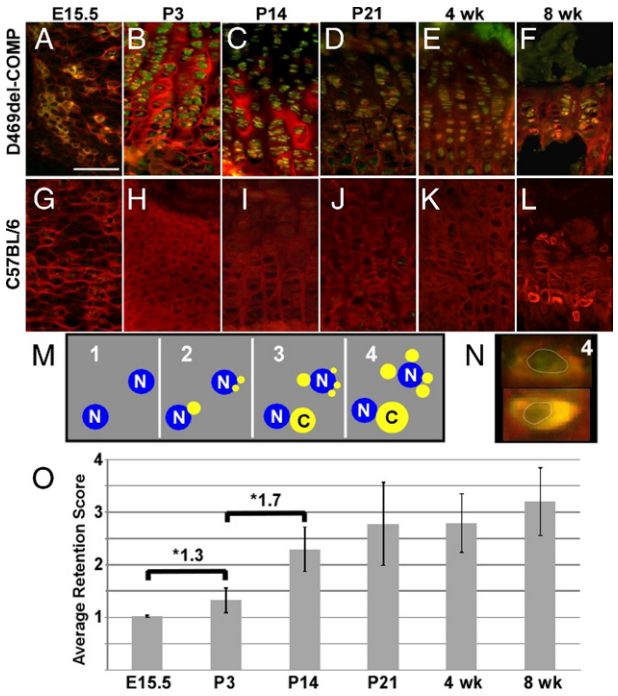

Figure 2. Intracellular retention of COMP in growth plates of D469del-COMP mice from E15 to 2 months of age. Immunostaining of D469del-COMP (**A–F**) and control C57BL/6 (**G–L**) growth plates with FLAG (green) and COMP (red) antibodies. Patchy intracellular retention (yellow indicates merged image) begins before birth at E15; progressive intracellular D469del-COMP accumulation is observed with increasing age. Control C57BL/6 growth plates show no intracellular retention of COMP. Original magnification, ×20 (**A–L**). **M:** Scoring methodology. A numerical score was assigned by visually comparing the cumulative size of D469del-COMP-positive rER cisternae with the area of the nucleus. C, retention; N, nucleus. **N:** Two examples of D469del-COMP growth-plate chondrocytes with a retention score of 4. **O:** Quantitation of progressive intracellular D469del-COMP in growth plates from E15 to 2 months of age. $^{*}P \leq 0.05$.

Cell Death Is Detected Only at P21 When Significant Intracellular D469del-COMP Retention Is Present

Previously we showed that expression of D469del-COMP in the mouse growth plate induces premature cell death.[44] Here, we define the onset and distribution of cell death using TUNEL staining (Figure 3, G–L and S–X). DAPI was used to localize the nucleus of each chondrocyte (Figure 3, A–F and M–R). Little or no cell death was seen in the D469del-COMP and control growth plates until P14, when it was restricted to the hypertrophic zone (Figure 3). A significant increase in cell death affecting chondrocytes throughout the D469del-COMP growth plate was seen at P21 and older ages (Figure 3, J–L). In contrast, in the control growth plates cell death was limited and restricted to the hypertrophic zone (Figure 3, V–X). Cell death correlated with the presence of significant accumulation of D469del-COMP in the growth-plate chondrocytes (Figure 3, J–L, and Figure 2, D–F). Levels of cell death remained high at 1 and 2 months of age (Figure 3, K, L, and Y), corresponding to fewer chondrocytes in the growth plate (Figure 1M). These results suggest that the level of intracellular retention of D469del-COMP induces cell death, which translates into significant loss of growth-plate chondrocytes.

Long Bones Are Significantly Reduced in D469del-COMP Mice

Finally, we assessed how loss of growth-plate chondrocytes affects the mouse skeleton. Radiographical measurements showed that the D469del-COMP tibia was wider and 12% shorter than the control tibia (Figure 4). The skeleton of D469del-COMP mice was smaller than that of the controls (Figure 5, A and B). The skull, snout, fore limbs, hind limbs, and phalanges of the D469del-COMP mouse were reduced, compared with controls (Figure 5, C,

E, G, I, and K). The rib cage was shortened, and there was a prominent sternum. These results indicate significant reduction in all of the bones derived from endochondral bone formation; the reductions were similar to those observed in pseudoachondroplasia patients.[24,40]

D469del-COMP Expression Induces a Proapoptotic Environment before D469del-COMP Retention and Cell Death Is Detected in the Growth Plate

To define the molecular mechanisms that contribute to intracellular retention and chondrocyte cell death, we analyzed the transcriptome from P1 and from 1-, 2-, 3-, and 4-week-old hind-limb knee joints from transgenic and control mice, using a microarray. Proapoptotic transcripts were modestly elevated, and antiapoptotic transcripts were slightly down-regulated at P1 (Table 1). Specifically, the transcripts from four prosurvival genes were expressed at lower levels in D469del-COMP P1 mice: *Bag3* (0.8×), *Bcl2* (0.6×), *Bcl2l1* (0.5×), and *Bcl2l2* (0.7×). In contrast, proapoptotic transcripts from five genes were up-regulated: *Casp8* (1.3×), *Bad* (1.6×), *Bax* (1.3×), and *Chop* (1.4 to 1.6×). Generally, expression of genes encoding proteins involved in generation of antioxidants and ROS were increased from 2 to 4 weeks (Table 1). Inflammatory gene expression spiked at 3 weeks of age in the D469del-COMP mice, which correlated with high levels of cell death in the growth plate (Figure 3 and Table 1).

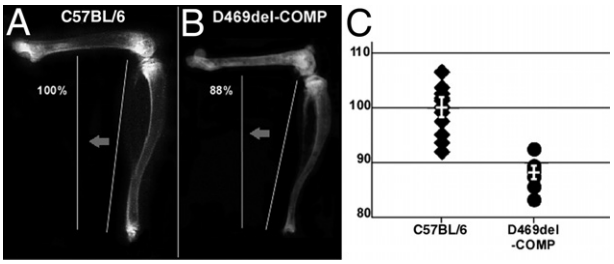

Figure 4. D469del-COMP limbs are shorter than C57BL/6 controls. **A** and **B:** Radiographs of hind limbs from 1-month-old C57BL/6 (**A**) and D469del-COMP (**B**) mice. **C:** Scatter plot of individual measurements. Horizontal bars indicate means, and error bars indicate ± SD. D469del-COMP mice have a 12% decrease in tibial length ($P < 0.000001$). Tibial measurements were taken from ≥12 limbs and the average length was calculated. A *t*-test was used to compare D469del-COMP tibial length to control.

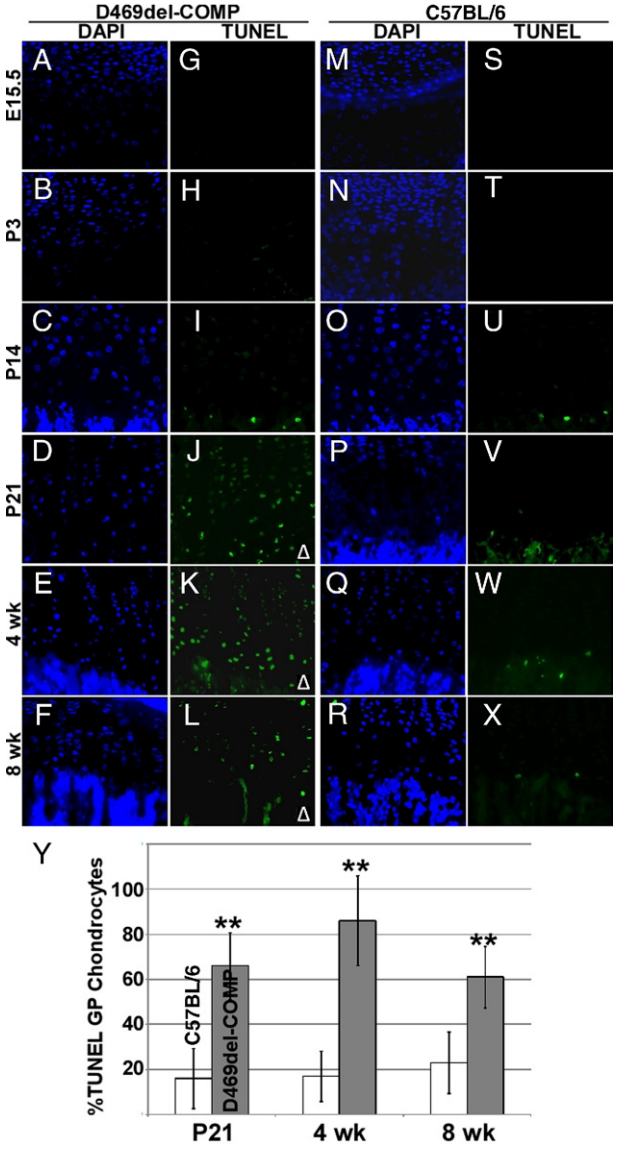

Figure 3. Chondrocyte cell death in D469del-COMP and control growth plates from mice at ages E15 to 2 months. TUNEL and DAPI staining of D469del-COMP (**A–L**) and control C57BL/6 (**M–X**) growth plates. Cell death in D469del-COMP and control growth plates is equivalent until P21, when D469del-COMP cell death is increased, compared with control (**J–L** and **V–X**). Original magnification, ×20 (**A–X**). **Arrowhead** indicates increase relative to control. **Y:** Quantitation of TUNEL-positive chondrocytes in growth plates from P21 to 2 months of age. Cell death in D469del-COMP growth plates is threefold higher at P21, fourfold higher at 1 month, and twofold higher at 2 months of age, compared with controls. $^{**}P \leq 0.01$.

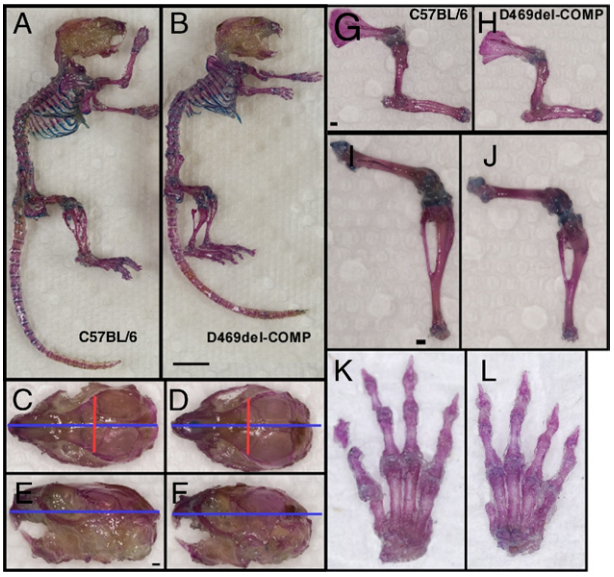

Figure 5. Skeletal elements of D469del-COMP and C57BL/6 control mice. **A** and **B:** Whole skeletal preparations of C57BL/6 control (**A**) and D469del-COMP (**B**) mice showing cartilage (Alcian Blue) and bone (Alizarin Red). **C–F:** Lateral and superior images of the skull of C57BL/6 (**C** and **E**) and D469del-COMP (**D** and **F**) mice. **G–J:** Fore and hind limbs of C57BL/6 (**G** and **I**) and D469del-COMP (**H** and **J**) mice. **K** and **L:** Front paws of C57BL/6 (**K**) and D469del-COMP (**L**) mice. Red and blue bars reflect skull measurements of a C57BL/6 mouse, for comparison with D469del-COMP mouse.

Table 1. Time-Dependent Altered mRNAs Involved in Cell Death, Oxidative Stress, and Inflammation in MT-COMP Mice

Genes	P1	1 week	2 weeks	3 weeks	4 weeks
Apoptosis: antiapoptotic					
Apip				2	1.6
Bag3	0.8				0.8
Bcl2	0.6		0.8		
Bcl2l1	0.5				
Bcl2l2	0.7	1.2			0.8
Bnip3l	1.2				1.2
Bcl2a1b		1.7	0.8		0.6
Bcl2a1d		2	0.8		0.7
Cfl1	1.6	1.3		0.3	
Apoptosis: caspase recruitment domain					
Casp1				1.5	
Casp6					0.8
Casp8	1.3			1.4	0.8
Nol3	1.5				
Apoptosis: proapoptotic					
Bax		1.3	0.6		0.8
Bad	1.6		0.8		
Apip					
Chop	1.4	1.6			
Antioxidants					
Epx				7	2
Ttn	0.5		1.7	0.6	
Mt3		1.9			
ROS metabolism					
Prg3				5	2
Prg2				4	1.7
Angptl7	0.2	3	0.4		0.6
Atox1	1.5				
Dusp1	0.6				1.6
Foxm1	1.5				
Glrx2				0.5	
Sepp1	0.7	0.8		1.6	1.8
Stk25	0.8				0.6
Inflammatory response					
Cd40		1.6		1.6	
Ly96		1.5			
Hdc	0.3			1.5	1.2
Pou2af1				4.2	
Cd79b				3.5	
Ear2	4			6.2	2
Ear3				5.2	2.6
Ear4				10.4	
Ear6				14.6	
Irf9	0.5			2.7	

Includes articular and growth-plate cartilage.

Other general trends in mRNA expression were found for genes involved in the UPR activation, ubiquitination, proteasome activation, DNA damage repair, and cell cycle regulation (Table 2). Expression of genes involved in protein folding and binding of unfolded proteins was elevated at P1 and depressed at 4 weeks. Ubiquitin ligase (E1) expression was elevated at P1; PSMB8, a component of the proteasome, was expressed at a higher level in 2- and 4-week-old D469del-COMP mice, compared with controls. mRNAs for proteins that bind to damaged DNA were elevated from P1 to 4 weeks, and DNA repair gene mRNAs were increased from P1 to 2 weeks

Table 2. Time-Dependent Expression Trends of Genes Involved in UPR, Ubiquitination, Proteasome, and DNA Damage in MT-COMP Mice

Gene	P1	P7	P14	P21	1 month
Protein folding, binding of unfolded protein	↑				↓
Ubiquitin ligase (E1)	↑				
Component of the proteasome PSMB8			↑		↑
Bind to damaged DNA	↑	↑	↑	↑	↑
DNA repair (*Chaf1a*, *Fen1*, *Polh*, *Ung*)	↑		↑		
Cell cycle control in response to DNA damage (*Gadd45a*, *Smc3*, *Rbbp4*)			↑		↑

Includes articular and growth-plate cartilage. ↑ indicates increased expression; ↓ indicates decreased expression.

(*Chaf1a*, *Fen1*, *Polh*, and *Ung*). Transcripts of genes that regulate the cell cycle in response to DNA damage were modestly increased at 2 and 4 weeks (*Gadd45a*, *Smc3*, and *Rbbp4*). Changes in mRNA expression of selected genes of the UPR, including *Chop*, *Gadd34*, and *Ero1B*, were confirmed using qRT-PCR analysis (data not shown). Taken together, these trends indicate that a pro-apoptotic environment is established early and that oxidative stress, DNA damage, and inflammation collectively promote chondrocyte cellular death. The observed changes in DNA damage response, UPR, and ubiquitin-proteasome mRNAs support this model.

D469del-COMP Is Not Retained in the Absence of Chop

Microarray transcriptome analysis showed a modest increase in Chop mRNA at P1 and P7 that was validated by qRT-PCR. Because Chop plays a significant role in UPR pathway and cell death, we generated a mouse line that expresses D469del-COMP on a *Chop*$^{-/-}$ background (Jackson Laboratory). The growth plates from these mice were analyzed at 1 month for intracellular retention of D469del-COMP, using a human COMP-specific antibody. In the absence of Chop, D469del-COMP was not retained in the chondrocyte, but was observed in a pericellular halo around the chondrocyte (Figure 6, G–I). However, as expected, D469del-COMP was distinctly evident within each chondrocyte in the D469del-COMP growth plate in mice expressing Chop (Figure 6, D–F), in contrast to controls (Figure 6, A and B).[44] Because the loss of Chop permits D469del-COMP to be exported, we asked whether the export of D469del-COMP alleviates other aspects of the pseudoachondroplasia chondrocyte pathology. We assessed proliferation and cell death by PCNA and TUNEL staining in the *Chop*$^{-/-}$ D469del-COMP growth plates at 1 month of age. We found that PCNA and TUNEL staining was significantly reduced in the *Chop*$^{-/-}$ D469del-COMP growth plate, compared with levels in the D469del-COMP mouse, but similar to levels in the control (Figure 6, J–O). Several inflammatory-related transcripts that were up-regulated in the D469del-COMP mice were down-regulated by twofold (Ear2, Ear3, Ear4, Ear6, and Irf9) in the *Chop*$^{-/-}$ D469del-COMP mice. These data indicate that these inflammatory-related transcripts are involved in the pseudoachondroplasia chondrocyte pathological process, consistent with the proposed model.

To further investigate the effects of the absence of Chop on ER stress genes, the expression of *Chop*, *Xbp1*, *Gadd45a*, *Gadd34*, *Ero1b*, *Grp78*, and *Edem1* was measured. D469del-COMP expression up-regulated the transcript level of *Chop*, *Xbp1*, *Gadd45a*, *Ero1b*, and *Grp78* in mice at 1 month of age, which was consistent with the microarray findings (Table 1 and Figure 7). In *Chop*$^{-/-}$ D469del-COMP mice, the expression of *Xbp1*, *Gadd45a*, and *Gadd34* was reduced, compared with D469del-COMP mice (Figure 7). These findings show that Chop plays a significant role in regulating the UPR genes that are up-regulated in D469del-COMP chondrocytes.

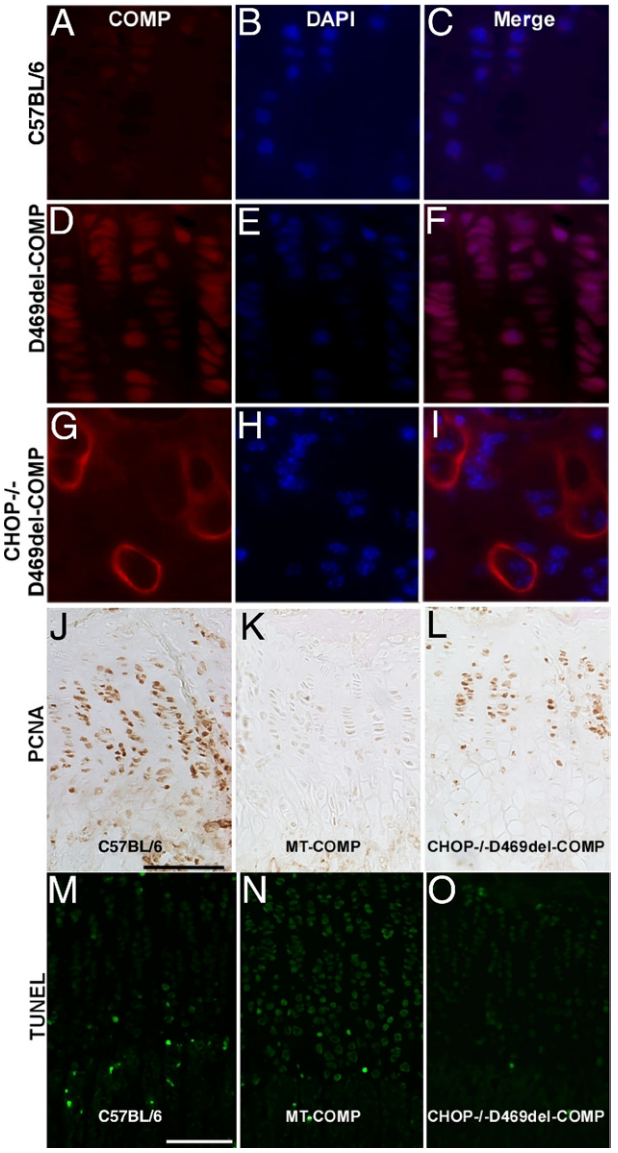

Figure 6. COMP immunostaining of C57BL/6, D469del-COMP, and *Chop* null D469del-COMP growth plates. DAPI staining marks the nucleus. A human specific COMP antibody (Abcam) was used. **A–I:** COMP and DAPI staining of C57BL/6, D469del-COMP, and *Chop*$^{-/-}$ D469del-COMP growth plates of 1-month-old mice. D469del-COMP was retained in all D469del-COMP chondrocytes (**D–F**) but had a pericellular distribution in the absence of Chop (**G–I**). **J–L:** PCNA immunostaining of growth plates of 1-month-old C57BL/6 (**J**), D469del-COMP (**K**), and *Chop*$^{-/-}$ D469del-COMP (**L**) mice. Decreased PCNA immunostaining is seen in D469del-COMP, compared with control and *Chop*$^{-/-}$ D469del-COMP mice. **M–O:** TUNEL immunostaining of growth plates of 1-month-old C57BL/6 (**M**), D469del-COMP (**N**), and *Chop*$^{-/-}$ D469del-COMP (**O**) mice. Increased number of apoptotic chondrocytes are found in D469del-COMP, compared with control and *Chop*$^{-/-}$ D469del-COMP growth plates. Original magnification, ×40 (**A–I**), ×20 (**J–O**).

D469del-COMP Increases Cell Death-Inducing Factor (AIF) and Phosphorylated Histone H2AX (γH2AX) Associated with Necroptosis

Our *in vitro* analysis of the UPR, stimulated by D469del-COMP, showed up-regulation of markers of necroptosis.[48] Necroptosis, a form of programmed death mediated through caspase-independent mechanisms, involves rupture of the plasma membrane.[49–52] To determine

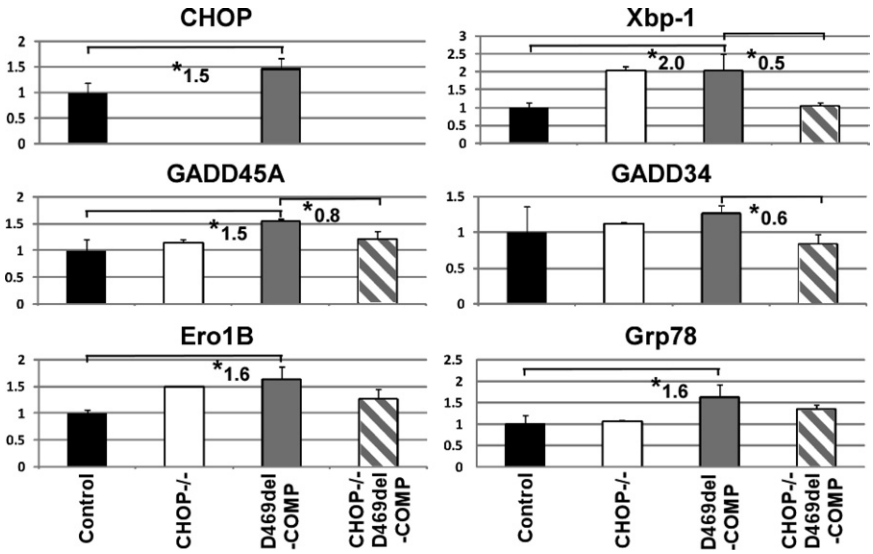

Figure 7. Loss of *Chop* reduces D469del-COMP-induced cellular stress. Quantitation of *Chop*, *Xbp1*, *Gadd45a*, *Gadd34*, *Ero1b*, and *Grp78* mRNAs from hind-limb joints of 1-month-old C57BL/6 (control), $Chop^{-/-}$, D469del-COMP, and $Chop^{-/-}$ D469del-COMP mice. D469del-COMP increases expression of specific ER stress mRNAs. The absence of *Chop* in the presence of D469del-COMP lowers the expression of these stress genes. $^{*}P < 0.05$.

whether the same mechanisms occur in the D469del-COMP growth plate, we assessed the level of AIF and γH2AX, which are associated with necroptosis. AIF is increased in the D469del-COMP growth plate at 1 month, compared with control (Figure 8, A–L). Additionally, cleaved AIF necessary for necroptosis execution was observed in the nucleus of D469del-COMP chondrocytes but not in controls. Moreover, γH2AX (the binding partner of AIF) was up-regulated in the D469del-COMP growth plate (Figure 8, M–O). Cleaved caspase 3 was not detected in either D469del-COMP or control growth plates (data not shown). Taken together, these findings indicate that D469del-COMP induces cell death in the growth-plate chondrocytes by necroptosis.

Discussion

COMP plays an important role in homeostasis of the growth plate and articular cartilage, but the exact function or functions still remain to be defined.[11–13,16,17,53,54] Absence of COMP causes mild perturbations in the growth plate, whereas D469del-COMP causes catastrophic effects, such as premature loss of chondrocytes, which translates into pseudoachondroplasia, a well-characterized form of dwarfism.[22,23,55] Despite cross-sectional information from iliac crest biopsies about growth plate disturbance in humans and transgenic mice expressing mutant COMP, the pathological processes in growth-plate chondrocytes resulting from D469del-COMP retention have not been characterized during development and growth. In the present study, we used doxycycline-inducible transgenic mice that express D469del-COMP in growth-plate chondrocytes to study the effects of D469del-COMP on growth-plate development. We show that, although D469del-COMP retention begins very early, before birth, it does not become pervasive until after birth, at which time it establishes a proapoptotic environment. Later in skeletal maturation, the pervasive D469del-COMP retention was associated with the onset of cell death and expression of mRNAs involved in ROS metabolism, antioxidant function, and inflammation. Importantly, by reducing the UPR Chop-mediated response, D469del-COMP was secreted from the chondrocytes, and the growth plate had a more normal appearance. These results have important implications for therapy.

Babies with pseudoachondroplasia have normal birth parameters, but show decreased linear growth by 2 years of age, and then very little long-bone growth after the age of 6 years. Mouse long-bone growth is essentially complete by 8 weeks, when the growth plate becomes quiescent. Similar to pseudoachondroplasia babies, the D469del-COMP mice appear normal at birth. However, the D469del-COMP mouse at 1 month had a dwarfed appearance, with an abnormal protuberant rib cage, similar to the human pectus carinatum seen in pseudoachondroplasia (Figure 5). There was significant reduction in long bones of the fore and hind limbs, with a 12% reduction in tibial length (Figure 4). Moreover, the digits in the fore limb were short (Figure 5). The face in pseudoachondroplasia is very angular, and the head circumference is normal. Similarly, the D469del-COMP mouse shows a reduction in snout length and a smaller cranial vault (Figure 5). Thus, we show that the D469del-COMP mice manifest most of the skeletal abnormalities of pseudoachondroplasia and truly mimic the human dwarfing condition.

Analysis of the growth plate showed that intracellular retention of D469del-COMP was limited to a few chondrocytes at E15.5. At birth (P1), intracellular retention of D469del-COMP had a patchy distribution in the growth plate that became extensive by P21 (Figure 2). Of note, only at P21 did gross growth plate changes become obvious, with fewer chondrocytes and reduced growth-plate width (Figures 1 and 3). The timing of cell death in the D469del-COMP growth plate followed the temporal pattern of intracellular retention, suggesting that significant retention in most growth-plate chondrocytes was necessary to induce cell death (Figure 3).

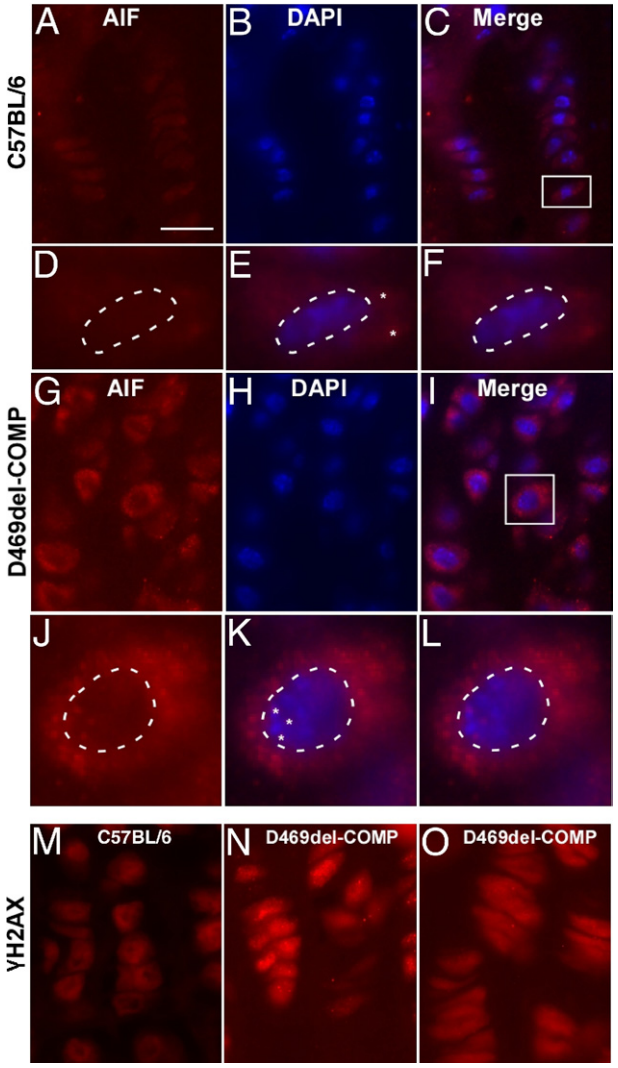

Figure 8. AIF and γH2AX immunostaining of C57BL/6 and D469del-COMP growth-plate chondrocytes. AIF and γH2AX antibodies were used to localize these necroptotic proteins; DAPI staining marks the nucleus. Dashed outlines mark the nucleus, regardless of stain. **A–L:** AIF and DAPI staining of C57BL/6 (**A–F**) and D469del-COMP (**G–L**) growth plates of 1-month-old mice. AIF was observed in the nucleus of D469del-COMP chondrocytes (**J–L**), but only in the cytoplasm of the controls (**D–F**). **Asterisks** mark AIF localization. **M–O:** γH2AX staining of C57BL/6 (**M**) and D469del-COMP (**N–O**) growth plates of 1-month-old mice. γH2AX was elevated in D469del-COMP growth plate, compared with control. Scale bar = 50 μm (A–C and G–I). Boxed area locates the image of a single nucleus, shown at higher magnification in the next row. Original magnification, ×20. **Inset** cells enlarged digitally.

To evaluate the processes contributing to chondrocyte cell death, transcriptome analysis was performed on hind-limb joints from mice at ages P1 to 4 weeks. Increases in proapoptotic genes (eg, *Chop*) and repressions of antiapoptotic factors (eg, Bcl-2 family) were found at P1 and P7, even though there was relatively little D469del-COMP retention. Despite the early apoptotic stimulus, D469del-COMP chondrocytes survived until 3 weeks, when D469del-COMP retention became widespread. Of note, select inflammatory markers showed a dramatic increase at that time point, but subsequently returned to normal values. In the *Chop*$^{-/-}$ D469del-COMP mouse, these same inflammatory transcripts were reduced two-fold, indicating that retained D469del-COMP elevates these inflammatory mRNAs but that D469del-COMP in the extracellular matrix does not. An increase in ROS metabolism genes and antioxidant genes coincided with the widespread cell death. ER stress is known to stimulate ROS production and oxidative stress, thereby causing inflammation.[56,57] Excessive and prolonged oxidative stress mediates cell death through caspase-independent mechanisms, and specifically through necroptosis.[58] Mild oxidative stress leads to caspase cleavage and apoptosis.[58] AIF, a necroptosis executioner, and its binding partner, γH2AX, were both elevated in D469del-COMP growth-plate chondrocytes (Figure 8). Our results show that at P1 to P7 apoptosis was stimulated when D469del-COMP retention and oxidative stress were minimal. However, necroptosis took over at 3 to 4 weeks, when extensive D469del-COMP retention generated excessive oxidative stress.

Studies in a mouse model of MED/EDM1 caused by a T585M COMP mutation suggested that Chop plays a role in mutant COMP-induced cell death.[42] This mouse showed little intracellular retention, but had increased apoptosis and decreased chondrocyte proliferation. Similarly, Chop mRNA was increased at P1 and P7 in our D469del-COMP mice, leading us to examine the effect of loss of Chop on the retention of D469del-COMP. Absence of Chop resulted in less retention of D469del-COMP, with export to the ECM (Figure 6). Importantly, the loss of Chop in the *Chop*$^{-/-}$ D469del-COMP mice results in an increase in proliferation and decrease in cell death, as assessed by PCNA and TUNEL staining, respectively (Figure 6). Additionally, expression of several stress-related genes were depressed in the *Chop*$^{-/-}$ D469del-COMP mouse, compared with the control mice (Figures 6 and 7). These results indicate that Chop-mediated cellular stress is a consequence of D469del-COMP retention, rather than of the presence of D469del-COMP in the extracellular matrix, as was previously suggested.[32,42] This also suggests that the ER quality control systems, particularly the Chop arm, prevent D469del-COMP export, and that by interrupting these sensing mechanisms D469del-COMP can be secreted.

Our unique transgenic mouse, which expresses D469del-COMP in a tissue-specific manner, is a substantial improvement over other models, because it recapitulates both the chondrocyte pathology and the skeletal abnor-

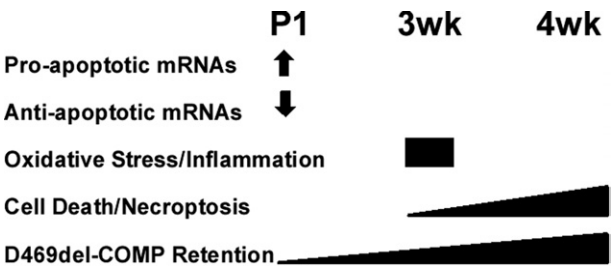

Figure 9. Schematic of D469del-COMP growth plate pathology during maturation of the mouse skeletal. Shortly after birth, there is little D469del-COMP intracellular retention and very little cell death. As retention increases, there is induction of oxidative stress and inflammation markers and abundant cell death occurs throughout the growth plate, rather than being limited to the hypertrophic zone.

malities associated with pseudoachondroplasia.[42–44,59] We show the progressive nature of D469del-COMP accumulation and chondrocyte loss, which now explains the deceleration of human long-bone growth in pseudoachondroplasia. Although COMP accumulation at birth is minimal, it steadily increases in all of the growth-plate chondrocytes. Chondrocytes are able to maintain normal function initially, but the D469del-COMP intracellular load subsequently appears to overwhelm the cellular coping systems, leading to cell death. These novel findings suggest a molecular model in which D469del-COMP triggers apoptosis signaling soon after birth (Figure 9). Later, when most chondrocytes are retaining D469del-COMP, oxidative stress leads to inflammation and DNA damage, and finally chondrocyte cell death occurs through necroptosis. Also shown is that Chop plays a significant role in the chondrocyte intracellular pathology. *Chop* and other proapoptotic mRNAs were elevated from P1 to P7, but antiapoptotic mRNAs were decreased. Despite unfavorable changes in apoptotic and survival mRNAs, growth-plate chondrocytes survived until P21, when all showed significant D469del-COMP intracellular retention and inflammation and ROS stress was triggered. Our results suggest that adverse molecular events occur before clinical diagnosis (at approximately 2 to 3 years of age in humans and by 3 weeks of age in mice). Therapeutics would be most effective if administered very early, before oxidative stress and inflammation responses are mounted. The tolerance of growth-plate chondrocytes to intracellular D469del-COMP may define a therapeutic window in which treatments would be the most effective before the initiation of inflammation and reactive oxygen stress.

Acknowledgments

We thank Trung Le and Francis Nguyen for technical assistance.

References

1. DiCesare PE, Mörgelin M, Mann K, Paulsson M: Cartilage oligomeric matrix protein and thrombospondin 1. Purification from articular cartilage, electron microscopic structure, and chondrocyte binding. Eur J Biochem 1994, 223:927–937
2. Hecht JT, Deere M, Putnam E, Cole W, Vertel B, Chen H, Lawler J: Characterization of cartilage oligomeric matrix protein (COMP) in human normal and pseudoachondroplasia musculoskeletal tissues. Matrix Biol 1998, 17:269–278
3. Hedbom E, Antonsson P, Hjerpe A, Aeschlimann D, Paulsson M, Rosa-Pimentel E, Sommarin Y, Wendel M, Oldberg A, Heinegård D: Cartilage matrix proteins. An acidic oligomeric protein (COMP) detected only in cartilage. J Biol Chem 1992, 267:6132–6136
4. Urban JP, Maroudas A, Bayliss MT, Dillon J: Swelling pressures of proteoglycans at the concentrations found in cartilaginous tissues. Biorheology 1979, 16:447–464
5. Kempson GE, Freeman MA, Swanson SA: Tensile properties of articular cartilage. Nature 1968, 220:1127–1128
6. Schmidt MB, Mow VC, Chun LE, Eyre DR: Effects of proteoglycan extraction on the tensile behavior of articular cartilage. J Orthop Res 1990, 8:353–363
7. Adams JC, Tucker RP, Lawler J: The thrombospondin gene family. Austin, TX, R.G. Landes, 1995
8. Fang C, Carlson CS, Leslie MP, Tulli H, Stolerman E, Perris R, Ni L, Di Cesare PE: Molecular cloning, sequencing, and tissue and developmental expression of mouse cartilage oligomeric matrix protein (COMP). J Orthop Res 2000, 18:593–603
9. Fang C, Johnson D, Leslie MP, Carlson CS, Robbins M, Di Cesare PE: Tissue distribution and measurement of cartilage oligomeric matrix protein in patients with magnetic resonance imaging-detected bone bruises after acute anterior cruciate ligament tears. J Orthop Res 2001, 19:634–641
10. Posey KL, Davies S, Bales ES, Haynes R, Sandell LJ, Hecht JT: In vivo human cartilage oligomeric matrix protein (COMP) promoter activity. Matrix Biol 2005, 24:539–549
11. Holden P, Meadows RS, Chapman KL, Grant ME, Kadler KE, Briggs MD: Cartilage oligomeric matrix protein interacts with type IX collagen, and disruptions to these interactions identify a pathogenetic mechanism in a bone dysplasia family. J Biol Chem 2001, 276:6046–6055
12. Mann HH, Ozbek S, Engel J, Paulsson M, Wagener R: Interactions between the cartilage oligomeric matrix protein and matrilins. Implications for matrix assembly and the pathogenesis of chondrodysplasias. J Biol Chem 2004, 279:25294–25298
13. Thur J, Rosenberg K, Nitsche DP, Pihlajamaa T, Ala-Kokko L, Heinegård D, Paulsson M, Maurer P: Mutations in cartilage oligomeric matrix protein causing pseudoachondroplasia and multiple epiphyseal dysplasia affect binding of calcium and collagen I, II, and IX. J Biol Chem 2001, 276:6083–6092
14. Rosenberg K, Olsson H, Mörgelin M, Heinegård D: Cartilage oligomeric matrix protein shows high affinity zinc-dependent interaction with triple helical collagen. J Biol Chem 1998, 273:20397–20403
15. Kipnes J, Carlberg AL, Loredo GA, Lawler J, Tuan RS, Hall DJ: Effect of cartilage oligomeric matrix protein on mesenchymal chondrogenesis in vitro. Osteoarthritis Cartilage 2003, 11:442–454
16. Xu K, Zhang Y, Ilalov K, Carlson CS, Feng JQ, Di Cesare PE, Liu CJ: Cartilage oligomeric matrix protein associates with granulin-epithelin precursor (GEP) and potentiates GEP-stimulated chondrocyte proliferation. J Biol Chem 2007, 282:11347–11355
17. Chen FH, Thomas AO, Hecht JT, Goldring MB, Lawler J: Cartilage oligomeric matrix protein/thrombospondin 5 supports chondrocyte attachment through interaction with integrins. J Biol Chem 2005, 280:32655–32661
18. Hecht JT, Makitie O, Hayes E, Haynes R, Susic M, Montufar-Solis D, Duke PJ, Cole WG: Chondrocyte cell death and intracellular distribution of COMP and type IX collagen in the pseudoachondroplasia growth plate. J Orthop Res 2004, 22:759–767
19. Hecht JT, Montufar-Solis D, Decker G, Lawler J, Daniels K, Duke PJ: Retention of cartilage oligomeric matrix protein (COMP) and cell death in redifferentiated pseudoachondroplasia chondrocytes. Matrix Biol 1998, 17:625–633
20. Merritt TM, Alcorn JL, Haynes R, Hecht JT: Expression of mutant cartilage oligomeric matrix protein in human chondrocytes induces the pseudoachondroplasia phenotype. J Orthop Res 2006, 24:700–707
21. Merritt TM, Bick R, Poindexter BJ, Alcorn JL, Hecht JT: Unique matrix structure in the rough endoplasmic reticulum cisternae of pseudoachondroplasia chondrocytes. Am J Pathol 2007, 170:293–300
22. Briggs MD, Hoffman SM, King LM, Olsen AS, Mohrenweiser H, Leroy JG, Mortier GR, Rimoin DL, Lachman RS, Gaines ES, Cekleniak JA, Knowlton RG, Cohn DH: Pseudoachondroplasia and multiple epiphyseal dysplasia due to mutations in the cartilage oligomeric matrix protein gene. Nat Genet 1995, 10:330–336
23. Hecht JT, Nelson LD, Crowder E, Wang Y, Elder FF, Harrison WR, Francomano CA, Prange CK, Lennon GG, Deere M, Lawler J: Mutations in exon 17B of cartilage oligomeric matrix protein (COMP) cause pseudoachondroplasia. Nat Genet 1995, 10:325–329
24. Unger S, Hecht JT: Pseudoachondroplasia and multiple epiphyseal dysplasia: new etiologic developments. Am J Med Genet 2001, 106:244–250
25. McKeand J, Rotta J, Hecht JT: Natural history study of pseudoachondroplasia. Am J Med Genet 1996, 63:406–410
26. Briggs MD, Chapman KL: Pseudoachondroplasia and multiple epiphyseal dysplasia: mutation review, molecular interactions, and genotype to phenotype correlations. Hum Mutat 2002, 19:465–478
27. Chen H, Deere M, Hecht JT, Lawler J: Cartilage oligomeric matrix protein is a calcium-binding protein, and a mutation in its type 3

repeats causes conformational changes. J Biol Chem 2000, 275:26538–26544
28. Chen TL, Stevens JW, Cole WG, Hecht JT, Vertel BM: Cell-type specific trafficking of expressed mutant COMP in a cell culture model for PSACH. Matrix Biol 2004, 23:433–444
29. Cooper RR, Ponseti IV, Maynard JA: Pseudoachondroplastic dwarfism. A rough-surfaced endoplasmic reticulum storage disorder. J Bone Joint Surg Am 1973, 55:475–484
30. Delot E, Brodie SG, King LM, Wilcox WR, Cohn DH: Physiological and pathological secretion of cartilage oligomeric matrix protein by cells in culture. J Biol Chem 1998, 273:26692–26697
31. DiCesare PE, Mörgelin M, Carlson CS, Pasumarti S, Paulsson M: Cartilage oligomeric matrix protein: isolation and characterization from human articular cartilage. J Orthop Res 1995, 13:422–428
32. Dinser R, Zaucke F, Kreppel F, Hultenby K, Kochanek S, Paulsson M, Maurer P: Pseudoachondroplasia is caused through both intra- and extracellular pathogenic pathways. J Clin Invest 2002, 110:505–513
33. Duke J, Montufar-Solis D, Underwood S, Lalani Z, Hecht JT: Apoptosis staining in cultured pseudoachondroplasia chondrocytes. Apoptosis 2003, 8:191–197
34. Ikegawa S, Ohashi H, Nishimura G, Kim KC, Sannohe A, Kimizuka M, Fukushima Y, Nagai T, Nakamura Y: Novel and recurrent COMP (cartilage oligomeric matrix protein) mutations in pseudoachondroplasia and multiple epiphyseal dysplasia. Hum Genet 1998, 103:633–638
35. Kleerekoper Q, Hecht JT, Putkey JA: Disease-causing mutations in cartilage oligomeric matrix protein cause an unstructured Ca2+ binding domain. J Biol Chem 2002, 277:10581–10589
36. Maddox BK, Mokashi A, Keene DR, Bächinger HP: A cartilage oligomeric matrix protein mutation associated with pseudoachondroplasia changes the structural and functional properties of the type 3 domain. J Biol Chem 2000, 275:11412–11417
37. Briggs MD, Mortier GR, Cole WG, King LM, Golik SS, Bonaventure J, Nuytinck L, De Paepe A, Leroy JG, Biesecker L, Lipson M, Wilcox WR, Lachman RS, Rimoin DL, Knowlton RG, Cohn DH: Diverse mutations in the gene for cartilage oligomeric matrix protein in the pseudoachondroplasia-multiple epiphyseal dysplasia disease spectrum. Am J Hum Genet 1998, 62:311–319
38. Hecht JT, Hayes E, Haynes R, Cole WG: COMP mutations, chondrocyte function and cartilage matrix. Matrix Biol 2005, 23:525–533
39. Hecht JT, Hayes E, Snuggs M, Decker G, Montufar-Solis D, Doege K, Mwalle F, Poole R, Stevens J, Duke PJ: Calreticulin, PDI, Grp94 and BiP chaperone proteins are associated with retained COMP in pseudoachondroplasia chondrocytes. Matrix Biol 2001, 20:251–262
40. Posey KL, Hayes E, Haynes R, Hecht JT: Role of TSP-5/COMP in pseudoachondroplasia. Int J Biochem Cell Biol 2004, 36:1005–1012
41. Hou J, Putkey JA, Hecht JT: Delta 469 mutation in the type 3 repeat calcium binding domain of cartilage oligomeric matrix protein (COMP) disrupts calcium binding. Cell Calcium 2000, 27:309–314
42. Piróg-Garcia KA, Meadows RS, Knowles L, Heinegård D, Thornton DJ, Kadler KE, Boot-Handford RP, Briggs MD: Reduced cell proliferation and increased apoptosis are significant pathological mechanisms in a murine model of mild pseudoachondroplasia resulting from a mutation in the C-terminal domain of COMP. Hum Mol Genet 2007, 16:2072–2088
43. Schmitz M, Niehoff A, Miosge N, Smyth N, Paulsson M, Zaucke F: Transgenic mice expressing D469Delta mutated cartilage oligomeric matrix protein (COMP) show growth plate abnormalities and sternal malformations. Matrix Biol 2008, 27:67–85
44. Posey KL, Veerisetty AC, Liu P, Wang HR, Poindexter BJ, Bick R, Alcorn JL, Hecht JT: An inducible cartilage oligomeric matrix protein mouse model recapitulates human pseudoachondroplasia phenotype. Am J Pathol 2009, 175:1555–1563
45. Tsumaki N, Tanaka K, Arikawa-Hirasawa E, Nakase T, Kimura T, Thomas JT, Ochi T, Luyten FP, Yamada Y: Role of CDMP-1 in skeletal morphogenesis: promotion of mesenchymal cell recruitment and chondrocyte differentiation. J Cell Biol 1999, 144:161–173
46. Marciniak SJ, Yun CY, Oyadomari S, Novoa I, Zhang Y, Jungreis R, Nagata K, Harding HP, Ron D: CHOP induces death by promoting protein synthesis and oxidation in the stressed endoplasmic reticulum. Genes Dev 2004, 18:3066–3077
47. Posey KL, Hankenson K, Veerisetty AC, Bornstein P, Lawler J, Hecht JT: Skeletal abnormalities in mice lacking extracellular matrix proteins, thrombospondin-1, thrombospondin-3, thrombospondin-5, and type IX collagen. Am J Pathol 2008, 172:1664–1674
48. Coustry F, Posey KL, Liu P, Alcorn JL, Hecht JT: Mutant COMP induces caspase-independent programmed cell death in rat chondrosarcoma cells. Am J Pathol 2012, 180:738–748
49. Golstein P, Aubry L, Levraud JP: Cell-death alternative model organisms: why and which? Nat Rev Mol Cell Biol 2003, 4:798–807
50. Artus C, Boujrad H, Bouharrour A, Brunelle MN, Hoos S, Yuste VJ, Lenormand P, Rousselle JC, Namane A, England P, Lorenzo HK, Susin SA: AIF promotes chromatinolysis and caspase-independent programmed necrosis by interacting with histone H2AX. EMBO J 2010, 29:1585–1599
51. Baritaud M, Boujrad H, Lorenzo HK, Krantic S, Susin SA: Histone H2AX: the missing link in AIF-mediated caspase-independent programmed necrosis. Cell Cycle 2010, 9:3166–3173
52. Vandenabeele P, Galluzzi L, Vanden Berghe T, Kroemer G: Molecular mechanisms of necroptosis: an ordered cellular explosion. Nat Rev Mol Cell Biol 2010, 11:700–714
53. Chen FH, Herndon ME, Patel N, Hecht JT, Tuan RS, Lawler J: Interaction of cartilage oligomeric matrix protein/thrombospondin 5 with aggrecan. J Biol Chem 2007, 282:24591–24598
54. Halász K, Kassner A, Mörgelin M, Heinegård D: COMP acts as a catalyst in collagen fibrillogenesis. J Biol Chem 2007, 282:31166–31173
55. Svensson L, Aszódi A, Heinegård D, Hunziker EB, Reinholt FP, Fässler R, Oldberg A: Cartilage oligomeric matrix protein-deficient mice have normal skeletal development. Mol Cell Biol 2002, 22:4366–4371
56. Santos CX, Tanaka LY, Wosniak J, Laurindo FR: Mechanisms and implications of reactive oxygen species generation during the unfolded protein response: roles of endoplasmic reticulum oxidoreductases, mitochondrial electron transport, and NADPH oxidase. Antioxid Redox Signal 2009, 11:2409–2427
57. Khaper N, Bryan S, Dhingra S, Singal R, Bajaj A, Pathak CM, Singal PK: Targeting the vicious inflammation-oxidative stress cycle for the management of heart failure. Antioxid Redox Signal 2010, 13:1033–1049
58. Hampton MB, Orrenius S: Redox regulation of apoptotic cell death. Biofactors 1998, 8:1–5
59. Posey KL, Liu P, Wang HR, Veerisetty AC, Alcorn JL, Hecht JT: RNAi reduces expression and intracellular retention of mutant cartilage oligomeric matrix protein. PLoS One 2010, 5:e10302